e-ISSN: 0976-822X, p-ISSN:2961-6042

Available online on http://www.ijcpr.com/

International Journal of Current Pharmaceutical Review and Research 2025; 17(10); 33-42

Original Research Article

Role of Magnetic Resonance Imaging in Evaluation of Cerebellopontine Angle Mass Lesions

Dimpal B. Sangat[1], Deepak Kumar Rajput[2], Kavita U. Vaishnav[3], Mahima T. Trivedi[4]

[1]Assistant Professor, Department of Radio-Diagnosis, Narendra Modi Medical College, Sheth L.G. General Hospital, Ahmedabad, Gujarat, India

[2]High Grade Professor, Department of Radio-Diagnosis, Narendra Modi Medical College, Sheth L.G. General Hospital, Ahmedabad, Gujarat, India

[3]Associate Professor, Department of Radio-Diagnosis, Narendra Modi Medical College, Sheth L.G. General Hospital, Ahmedabad, Gujarat, India

[4]2nd Year Radiology Resident, Department of Radio-Diagnosis, Narendra Modi Medical College, Sheth L.G. General Hospital, Ahmedabad, Gujarat, India

Received: 01-07-2025 / Revised: 16-08-2025 / Accepted: 01-09-2025
Corresponding Author: Dr. Mahima T. Trivedi
Conflict of interest: Nil

Abstract

Background: Cerebellopontine angle (CPA) masses are the most common neoplasm in the posterior fossa, accounting for 5%-10% of intracranial tumors. MRI is considered the gold-standard method for the diagnosis of cerebellopontine angle lesions and describing the imaging feature of CPA masses.

Aim and Objectives: To evaluate the role of magnetic resonance imaging (MRI) aided with contrast-enhanced MRI in the evaluation of cerebellopontine angle mass lesions.

Materials and Methods: A prospective, single-center observational study was conducted over period of 18 months (JAN 2024–JUNE 2025) at a tertiary care hospital. The study included total of 30 patients with lesions of cerebellopontine angle were referred to radiology departments for MRI. All patients included were subjected to a detailed physical examination followed by MRI scan using a siemens MRI scanner with a standardized protocol. Contrast study was used to characterize the mass lesions.

MRI findings were analyzed with respect to lesion morphology, signal characteristics, and diffusion restriction. Data on patient demographics, clinical symptoms, and detailed MRI findings were systematically collected and analyzed.

Results: Most common tumors of CPA are vestibular schwannomas; second most frequent CPA tumors are meningiomas. Epidermoid cyst and arachnoid cysts are less common CPA tumors. In our study, there were 11 cases of vestibular schwannomas, 9 cases of meningiomas, 6 cases of epidermoid cysts, 3 cases of arachnoid cysts and 1 case of lipoma.

The highest number of cerebellopontine angle masses was found in the age group between 31 and 40 years with slight male predominance. The most common presenting symptom was headache, followed by vertigo and hearing loss.

Conclusion: The most common CPA mass was vestibular schwannoma followed by meningioma and epidermoid cyst. Magnetic resonance imaging is more sensitive and more specific in diagnosing cerebellopontine angle mass.

Keywords: Cerebellopontine, Mass, Schwannoma, Magnetic Resonance.

Introduction

Lesions of the cerebellopontine angle (CPA) comprise 10% of all intracranial tumours. The cerebellopontine angle (CPA) cistern is a subarachnoid space centered within the posterior cranial fossa at the level of the internal auditory canal and is bounded by the pons, the anterior aspect of the cerebellum and the petrous temporal bone covered by dura mater. It contains the short intracranial courses of the fifth, seventh, and eighth cranial nerves. [1]

Cerebellopontine angle (CPA) lesions are usually benign and clinically non-specific or asymptomatic or it may present with headache, vertigo, tinnitus, or unilateral hearing loss. The presenting symptoms depending upon the site of tumor origin, nature of the lesion and displacement or involvement of the neurovascular and cerebral structure by the lesions.

[2] Therefore, preoperative diagnosis of a CPA region tumor is mainly based on imaging. Most common extra-axial tumors of CPA are vestibular schwannomas, which constitutes the about 70-80% of all CPA lesions. Meningiomas are the second most common lesion in this location. Other lesions may be congenital masses of the CPA (epidermoid, arachnoid cysts and lipomas); may originate from the adjacent cerebellum or brainstem (such as gliomas or parenchymal metastases), the vessels in the posterior fossa (arteriovenous malformations or aneurysms), and the adjacent temporal bone (Paget disease); or may be related to systemic leptomeningeal processes (infection or inflammatory processes, such as meningitis). [3,4]

MRI has excellent soft tissue contrast resolution and is the preferred imaging modality for differentiation and characterization of various soft tissues and fluids. In addition to conventional MR sequences of the brain, current imaging evaluation of the CPA includes high-resolution heavily T2-weighted imaging, such as constructive interference in steady-state (CISS), fast imaging employing steady-state acquisition (FIESTA) are helpful. Diffusion-weighted imaging (DWI) has been utilized for temporal bone and CPA imaging, particularly when abscesses or epidermoid are suspected. [5]

Magnetic resonance (MR) imaging characteristics of the different CPA lesions (including anatomic site of origin, shape, density, signal and behavior after contrast media injection), as well as provide data from MR advanced techniques such as MR spectroscopy, when available, as they may bring crucial new data that allow accurate preoperative diagnosis.

The purpose of this study is to elucidate the pivotal and comprehensive role of MRI in the assessment of a wide array of cerebellopontine angle lesions. We aim to correlate the specific MRI findings with clinical presentations to establish its utility in diagnosing cerebellopontine angle lesions, thereby providing a crucial roadmap for surgical planning and improving patient outcomes.

Materials and Methods

Study design, duration, and setting: A prospective, single-center observational study was conducted in the Department of Radio-Diagnosis at Narendra Modi Medical College & L.G. Hospital, Ahmedabad, over a period of 18 months from JAN 2024 to JUNE 2025. Informed consent was taken from all patients undergoing this study. Data were kept confidential and used exclusively for research purposes.

Sample size and sampling: The study included total of 30 patients with malignant lesions of cerebellopontine angle and were referred to radiology departments for MRI.

All patients included were subjected to a detailed physical examination followed by MRI scan using a siemens MRI scanner with a standardized protocol.

Inclusion Criteria: All patients referred with clinical suspicion and presented with signs and symptoms suggestive of any lesion in the cerebellopontine angle were included.

Exclusion Criteria: Patients who did not provide consent for participation were excluded. Critically ill patient and patient with history of previous surgical intervention were excluded. Those with any contraindication to undergo MRI.

Study procedures and MRI Protocol: All MRI examinations were performed on a Siemens Magnetom Essenza 1.5 Tesla whole-body scanner. The protocol included: T2-weighted image (T2WI) axial, sagittal and coronal planes, T1-weighted image (T1WI) axial, coronal and sagittal plane, fluid-attenuated inversion recovery (FLAIR) axial and coronal, Diffusion-weighted imaging (DWI) axial and constructive interference in steady state (CISS) axial images were taken. For contrast studies, gadopentate dimeglumine (0.1 mmol/kg body weight) was administered intravenously. Post-contrast T1WI was obtained in axial, sagittal, and coronal planes.

Data Collection and Analysis: Relevant clinical data, including history and examination findings of all the patients were correlated. Additional imaging (radiographs, CT) were correlated when available. Data on patient demographics, clinical symptoms, and detailed MRI findings were systematically collected and analyzed using descriptive statistics. The results were expressed in percentages, and data were presented in tables and graphs.

Results and Observations

Table 1: Distribution of CPA Tumors

Pathology	No. of Cases	Percentage (%)
Vestibular Schwannoma	11	36.7
Meningioma	9	30.0
Epidermoid Cyst	6	20.0
Arachnoid Cyst	3	10.0
Lipoma	1	3.3

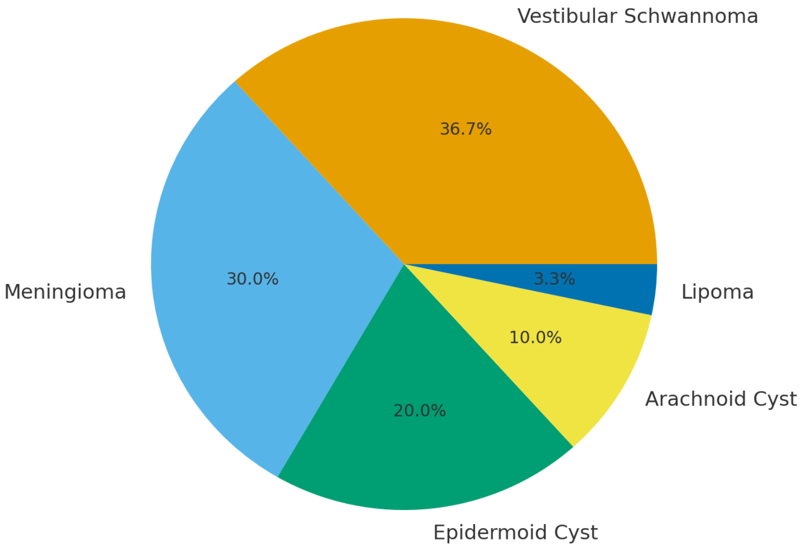

Figure 1: Distribution of CPA Tumors

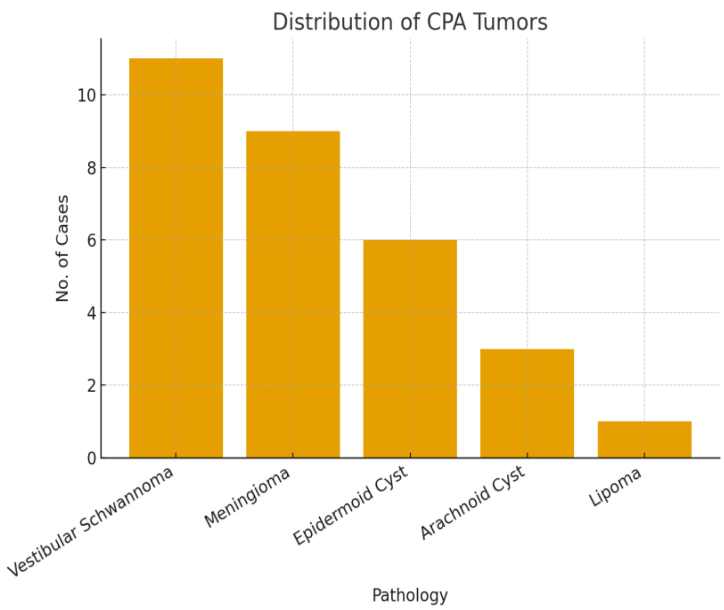

Figure 2: Distribution of CPA Tumors

The pie chart and bar chart provides a visual representation of the distribution. Vestibular schwannoma being the largest group accounted for 36.7 % of the cases, cases of meningioma made up 30 %, epidermoid cyst made up 20%, arachnoid cyst made up 10%, while lipoma constituted 3.3% of cases.

Table 2: Age Distribution of CPA Masses

Age Group	No. of Cases	Percentage (%)
21-30	7	23.3
31-40	10	33.3
41-50	7	23.3
51-60	4	13.3
61-70	2	6.7

Table 3: Gender Distribution of CPA Masses

Gender	No. of Cases	Percentage (%)
Male	17	56.7
Female	13	43.3

Table 4: Predominant Symptoms of CP Angle Mass (n = 30)

Predominant Symptoms	No. of Patients	Percentage (%)
Headache	12	40.0
Vertigo	8	26.7
Hearing Loss	6	20.0
Tinnitus	2	6.7
Imbalance / Ataxia	1	3.3
Facial Numbness/Weakness	1	3.3
Total	30	100%

Table 5: T1 Characteristics of CPA Lesions

Pathology	Hypointense	Isointense	Hyperintense
Vestibular Schwannoma	11	0	0
Meningioma	5	4	0
Epidermoid Cyst	4	2	0
Arachnoid Cyst	3	0	0
Lipoma	0	0	1

Table 6: T2 Characteristics of CPA Lesions

Pathology	Hypointense	Isointense	Hyperintense
Vestibular Schwannoma	0	0	11
Meningioma	0	2	7
Epidermoid Cyst	0	0	6
Arachnoid Cyst	0	0	3
Lipoma	0	0	1

Table 7: FLAIR Characteristics of CPA Lesions

Pathology	Hypointense	Hyperintense
Vestibular Schwannoma	0	11
Meningioma	0	9
Epidermoid Cyst	6	0
Arachnoid Cyst	3	0
Lipoma	0	1

Table 8: DWI Characteristics of CPA Lesions Diffusion restriction

Pathology	Present	Absent
Vestibular Schwannoma	11	0
Meningioma	9	0
Epidermoid Cyst	6	0
Arachnoid Cyst	0	3
Lipoma	0	1

Table 9: Post-contrast Characteristics of CPA Lesions

Pathology	Homogeneous Enhancement	Heterogeneous Enhancement	No Enhancement
Vestibular Schwannoma	0	11	0
Meningioma	8	1	0
Epidermoid Cyst	0	0	6
Arachnoid Cyst	0	0	3
Lipoma	0	0	1

Interpretation of Results

In the present study of 30 patients with CPA lesions, vestibular schwannoma emerged as the most common pathology (36.7%), followed by meningioma (30%) and epidermoid cyst (20%). Less common lesions included arachnoid cysts (10%) and lipoma (3.3%). This distribution aligns with published literature where vestibular schwannoma and meningioma are consistently reported as the predominant CPA masses. Demographic analysis showed a peak incidence in the 31–40 years age group (33.3%), with a slight male predominance (56.7%). The age and gender profile broadly reflects known patterns of occurrence of these tumors. Clinical presentation was dominated by headache

(40%), followed by vertigo (26.7%) and hearing loss (20%), while less frequent symptoms included tinnitus, imbalance/ataxia, and facial weakness. This highlights the overlap of CPA lesion symptoms with other neurological and otologic disorders, underscoring the importance of imaging in early diagnosis. On MRI characterization, vestibular schwannomas typically appeared T1 hypointense and T2 hyperintense with heterogeneous post-contrast enhancement. Meningiomas showed iso- to hypo-intensity on T1, iso- to hyperintensity on T2 and demonstrated predominantly homogeneous enhancement, consistent with their extra-axial dural origin. Epidermoid cysts were characteristically T1 hypointense, T2 hyperintense, FLAIR hypointense with dirty signal, and showed diffusion restriction, without post-contrast enhancement, making DWI an important tool in differentiating them from arachnoid cysts. Arachnoid cysts were distinguished by their CSF-like intensity across all sequences and lack of enhancement. Lipomas demonstrated intrinsic T1 hyperintensity with no enhancement, typical of their fat content. Overall, MRI played a crucial role not only in detecting CPA lesions but also in their tissue characterization and differentiation, guiding appropriate clinical and surgical management.

Discussion

Vestibular schwannoma: Vestibular schwannoma is by far the most frequent tumor in the CPA, accounting for 70% to 80% of all CPA masses. Most vestibular schwannomas develop from the Schwann sheath of the inferior vestibular nerve in the IAC where they grow slowly. Then, they smoothly erode the posterior edge of the porus acusticus and may give rise to a round or oval component in the CPA cistern, thus giving the typical "ice cream on cone" pattern. [6,7] Intracranial schwannomas occur in all the age groups, but the peak incidence is in the fourth to seventh decades of life. There is a distinct sex predilection with a female-to-male ratio of 2:1. The typical presentation is with adult-onset sensorineural hearing loss or non-pulsatile tinnitus. The symptom of vestibular schwannomas depends upon the size and location of the tumor. When it is in the intracanalicular stage it may present as a unilateral sensorineural hearing loss, tinnitus, or vertigo. In cisternal stage, it worsens the hearing loss, tinnitus, disequilibrium, and possible headache. When tumor progresses further, it compresses the brainstem and trigeminal symptoms may also develop. Further progress of the tumor causes pressure on the fourth ventricle with obstructive hydrocephalus, facial weakness, headache, vision loss, or diplopia may occur.

MRI is the very good modality to detected small tumors, especially within the IAC, because of the lack of bone-induced artifact and the multidimensional capability of this modality. Tumors < 5 mm in diameter can be reliably identified on CISS images, appearing mild homogenously hypo or iso-intense (to adjacent brain) ovoid or tubular intracanalicular masses, hypointense on T1WI with intense homogeneous contrast-enhancement. On T2W sequences, they appear mildly to markedly hyperintense and may be obscured by the similarity in signal intensity to that of the surrounding cerebrospinal fluid (CSF). In larger tumors, intratumoral degenerative changes may result in an increase in heterogeneity of signal. On axial images, the tumor often has a comma-like shape with a globular cisternal mass medially and a short tapered fusiform extension laterally into the IAC. Compression and displacement of the adjacent cerebellar hemisphere, pons, or medulla may occur as the tumor enlarges. Heterogeneous contrast-enhancement is seen in the most of the cases. The differential diagnosis is meningioma and epidermoid tumor. [8,9.10]

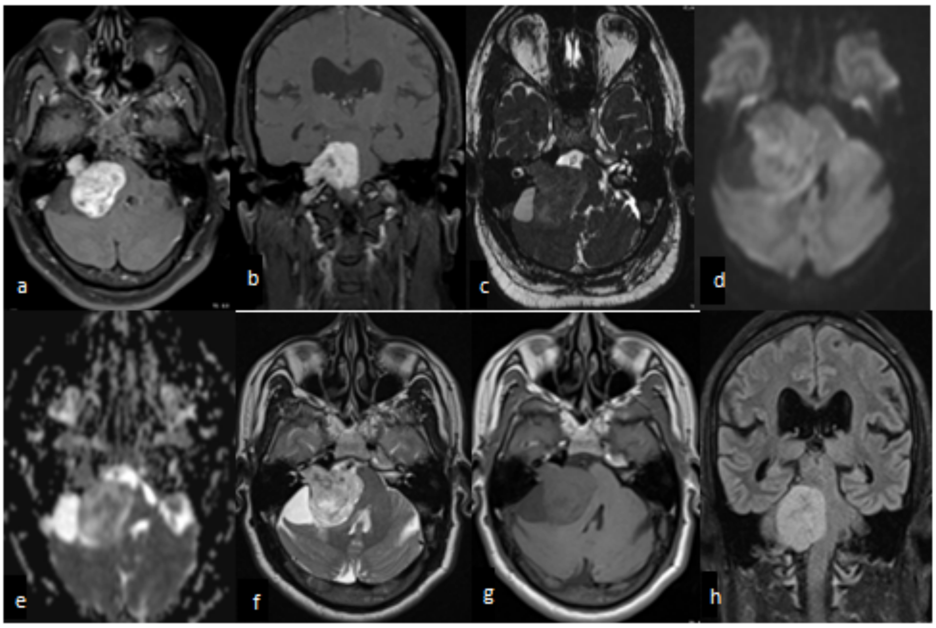

Figure 3: Large vestibular schwannoma in patient presenting with dizziness, right deafness and chronic headache (a,b) Contrast enhanced axial and coronal T1-weighted image and (c) Constructive interference in steady state axial image and shows typical "ice cream on-cone" CPA mass lesion that heterogeneously enhances. The component enlarging the porus of the internal auditory canal is very suggestive of the diagnosis. (d,e) The lesion show heterogeneous diffusion restriction. (f) T2-weighted imaging showing right sided cerebellopontine angle intracanalicular tumor compressing the pons, 4^{th} ventricle and adjacent cerebellar hemisphere. (g) It is hypointense on T1-weighted imaging and (h) hyperintense on FLAIR

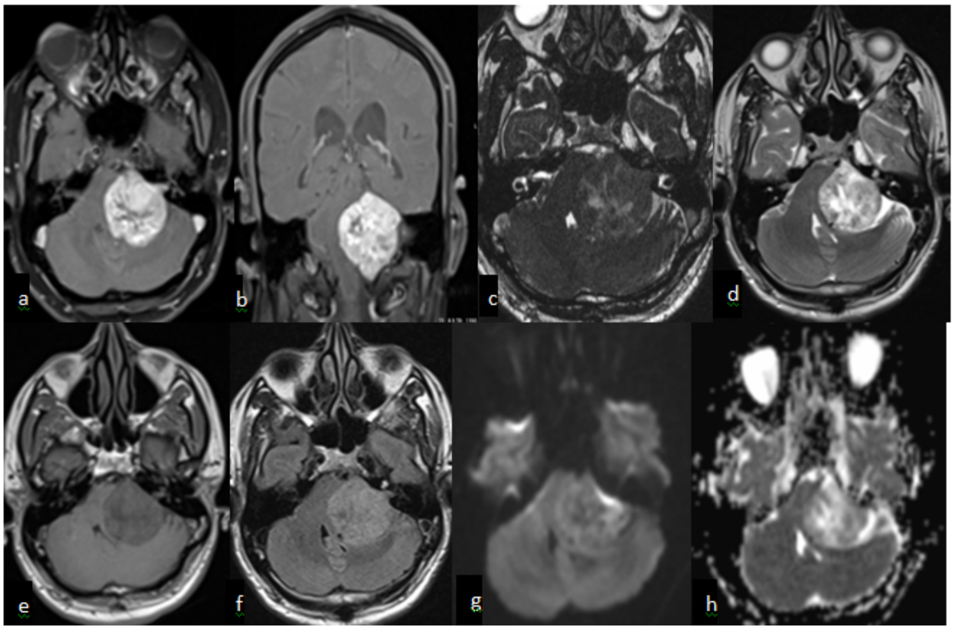

Figure 4: Vestibular schwannoma in patient presenting with left sided hearing loss, vertigo and headache. (a,b) Axial and coronal post-contrast T1-weighted image demonstrates a heterogeneously enhancing mass lesion shows typical "ice cream on-cone appearance" with a central non-enhancing region located in the left cerebellopontine angle. The mass widens the left porus acousticus and extends into the left internal auditory canal. There is associated mass effect upon the pons and cerebellar peduncle with significant compression of the fourth ventricle. (c) Constructive interference in steady state axial image shows left CPA mass lesion with intracanalicular extension (d) T2-weighted axial imaging showing left sided heterogenous cerebellopontine angle lesion with internal hypointense areas. (e) It is hypointense on T1-weighted imaging and (f) relatively hyperintense on FLAIR. (g,h) The lesion show heterogeneous diffusion restriction

Meningioma: Meningioma is the most common intracranial extra-axial tumor in adults, but is the second most frequent lesion in the CPA after vestibular schwannoma, representing 10%–15% of all tumors in this location. Meningiomas are solid, well-circumscribed, and slow-growing tumors that arise from arachnoid meningothelial cells and grow slowly in the CPA, independently from the internal auditory canal. Common sites are in the frontal and parietal convexities and the parasagittal region (in close association with the falx cerebri. In CPA they are usually located at the posterior aspect of the temporal bone or at the premeatal area, from where they can easily extend into the IAC, but without enlarging the porus. They occur with a peak incidence in the fifth through seventh decades of life. Meningiomas occur preponderantly in females. The most frequent initial complaints were hearing loss, tinnitus and headache. MRI clearly depicts a broad-based dural hemispheric or oval lesion with homogeneous appearance, attached to the petrous dura mater or the inferior aspect of the tentorium. On T1WIs, they appear iso- to hypo-intense to the adjacent cerebral cortex. On T2WIs, about 50% are mildly hyperintense relative to adjacent gray matter and 50% are isointense to the cortex. It is hypointense on CISS sequence obliterating the vestibulocochlear nerve. Meningiomas are strongly homogeneously enhance on postcontrast T1WI. Though not specific to meningiomas, the intense enhancement of the non-neoplastic thickened peritumoral dura, the so-called "dural tail sign", is particularly frequent in association with meningiomas and should suggest the diagnosis when observed. [11,12,13]

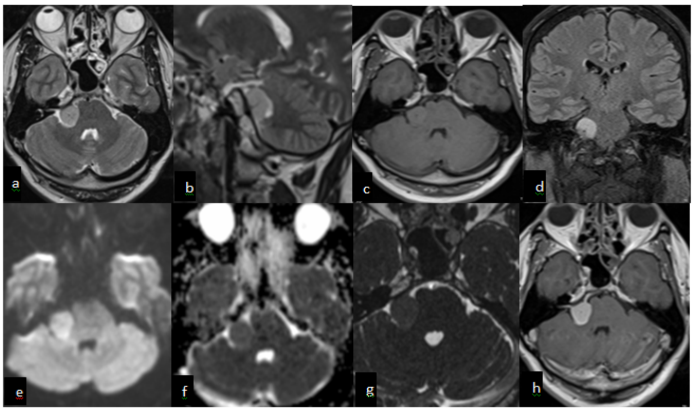

Figure 5: Right cerebellopontine angle meningioma presenting with chronic headache, tinnitus and dizziness. (a,b) Axial and sagittal T2-weighted image demonstrates small round dural based solid mass lesion in right cerebellopontine angle region (c) the lesion appears iso on T1-weighted imaging and (d) hyperintense on FLAIR images. (e,f) The lesion show homogenous diffusion restriction. (g) Constructive interference in steady state axial image shows well defined right CPA mass lesion (f) Axial post-contrast T1-weighted image shows vivid and homogeneous contrast enhancement of the mass. The lesion shows mass effect over pons and cerebellar peduncle

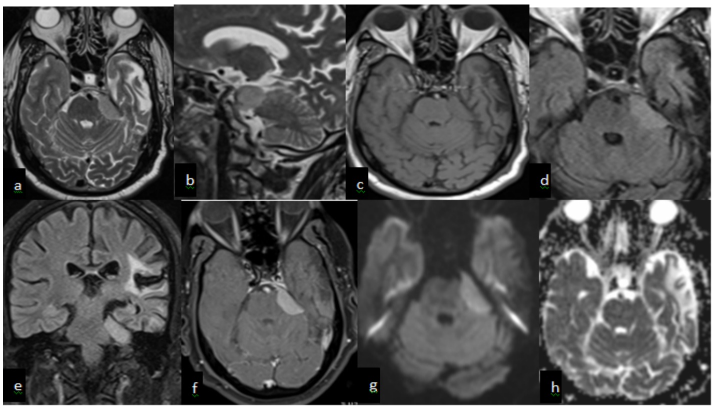

Figure 6: Left CPA meningioma in a patient present with dizziness and left sensorineural hearing loss. (a,b) Axial and sagittal T2-weighted image demonstrates dural based solid mass lesion in left cerebellopontine angle region (c) the lesion appears iso to hypointense on T1-weighted imaging and (d,e) relatively hyperintense on axial and coronal FLAIR images.(f) Axial post-contrast T1-weighted image shows intense homogeneous contrast enhancement of the mass with a broad base dural attachment. The lesion shows minimal mass effect over pons. (g) Axial diffusion-weighted image and the (h) corresponding apparent diffusion coefficient (ADC) map show associated restricted diffusion

Epidermoid Cysts

Epidermoid cysts are the third most common tumor of the CPA, accounting for 5% of all lesions in this location and 1% of all intracranial tumors. These are congenital lesions arising from the inclusion of ectodermal epithelial tissue during neural tube closure. The most common locations include the brainstem, pituitary gland, and in the posterior fossa along the cerebellum and brainstem. These lesions tend to encase and surround (and not displace) adjacent structures, such as cranial nerves and vessels in the CPA. Typically patients are between 20 and 40 years of age. There may be increased prevalence in males. A unique clinical presentation of epidermoid cysts is recurrent episodes of aseptic meningitis related to inflammation induced by the keratin debris.

On MRI epidermoid cysts demonstrate imaging characteristics and a signal intensity similar to that of CSF. On T1WIs, slightly hyper- or iso-intense relative to the gray matter and isointense relative to CSF on T2WIs, but they may be slightly hyperintense. Fluid-attenuated inversion recovery (FLAIR) images are useful in distinguishing these lesions from the CSF normally located in the CPA, as signal is incompletely suppressed in an epidermoid cyst. On DWI presence it shows restricted diffusion, which is useful in initial evaluation of residual tumor in postoperative patient and differentiating epidemoid and arachnoid cysts. Epidermoid cyst show restricted diffusion on DWI. It does not enhance on postcontrast T1WI. [14,15,16,17]

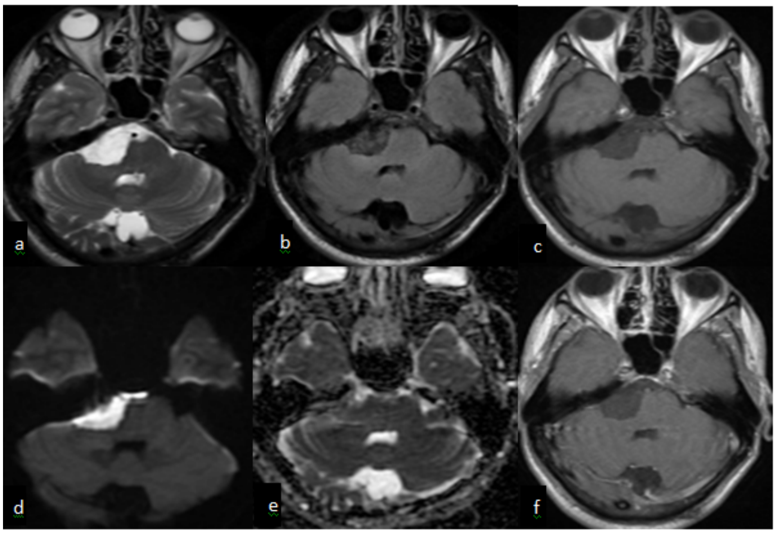

Figure 7: Epidermoid cyst of right cerebellopontine angle. (a) Axial T2-weighted imaging showed hyperintense lesion occupying the right cerebellopontine angle. The lesion causing mild mass effect over right side of pons (b) It is hypointense with dirty signal on FLAIR imaging and (c) hypointense on T1 weighted image (d,e) it showed restriction on diffusion weighted imaging, (f) Axial post-contrast T1-weighted image shows no post contrast enhancement

Arachnoid Cysts: Arachnoid cysts are benign, congenital, intra arachnoidal space-occupying lesions account for less than 1% of lesions in the CPA. Most arachnoid cysts are supratentorial in location, most commonly in the middle cranial fossa (50-60% of lesions). Other locations include the suprasellar cistern and posterior fossa (10%), where they occur most commonly in the CPA cistern. Arachnoid cysts are usually asymptomatic it can give symptoms when they enlarge resulting the mass effect. Large arachnoid cyst at CPA can compress the vestibulocochlear nerve and present with tinnitus or hearing loss, when it compress pons can present vertigo.

On imaging, MRI is the diagnostic technique of choice as it can demonstrate the exact location, extent, and the relationship of the arachnoid cyst to the adjacent brain or spinal cord. On MRI, arachnoid cysts appear as well-defined intracranial masses that follow CSF intensity on all sequences. Differentiation from epidermoid cysts is made by the complete absence of signal on FLAIR images and by lack of diffusion restriction on DWI. Arachnoid cysts shows no enhancement with gadolinium. [17,18,19]

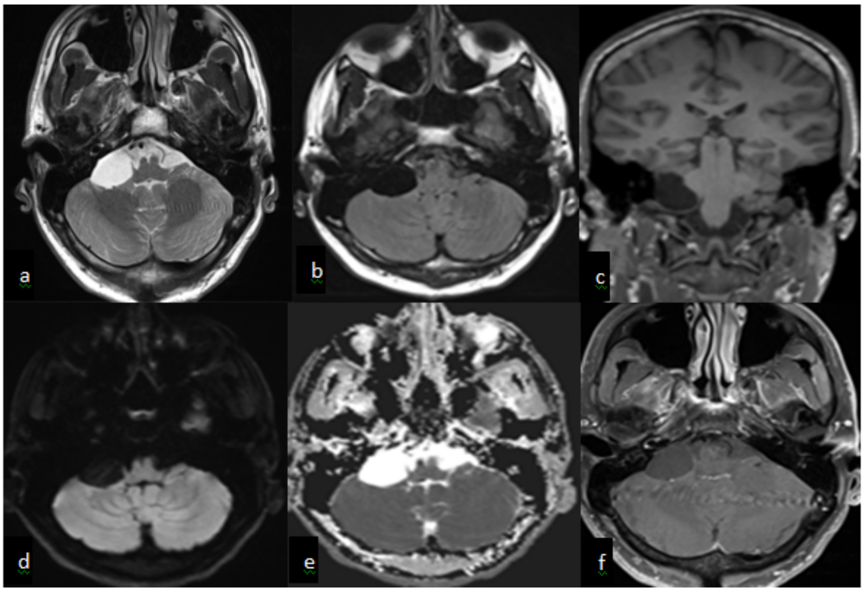

Figure 8: Arachnoid cyst. (a) Axial T2-weighted, (b) axial FLAIR imaging images and (c) coronal T1-weighted showing a well-defined cerebrospinal fluid signal intensity lesion at right cerebellopontine angle, (d) Axial diffusion-weighted image and the (e) corresponding apparent diffusion coefficient (ADC) map show no restricted diffusion. (f) On post contrast T1-weighted sequences no contrast enhancement

Lipoma: Intracranial lipomas are benign lesions consisting of adipose tissue that originate from congenital malformations of the meninges. CPA lipomas account for around 10% of all intracranial lipomas. CPA lipomas are homogeneous fatty lesions, tend to exhibit an infiltrative growth pattern within the neurovascular structures due to their developmental origin. Characteristically lipomas of the CPA have the trigeminal nerve, facial nerve and vestibulocochlear nerve coursing through it with the latter two on their way to the internal auditory canal. They are often asymptomatic. Due to their location and the associated cranial nerves, if symptomatic, patients commonly present with trigeminal neuralgia, facial symptoms, hearing deficit, vertigo or tinnitus.

On MRI lipomas appear as homogeneous high signal intensity on T1WIs, which decreases on fat-suppressed images. No post contrast enhancement after contrast media administration and can produce blooming on SWI due to susceptibility artifact. [20,21,22]

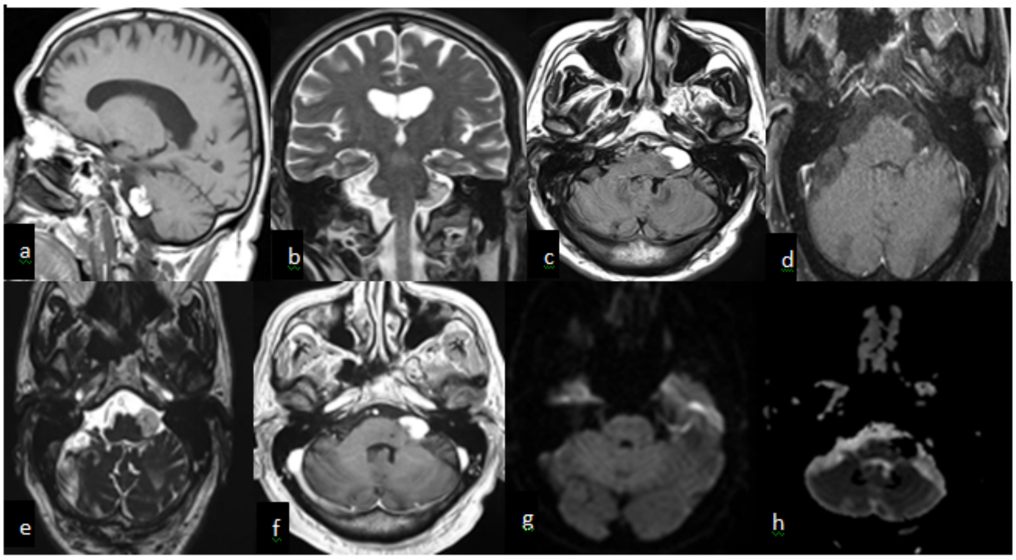

Figure 9: Left CPA lipoma. (a,b,c) well defined mass lesion shows a high signal on T1, T2 and FLAIR with (d) signal dropout on fat suppressed t1 weighted post contrast sequence with low signal margin on steady state axial image. (e) no post contrast enhancement of T1 weighted post contrast images. (f,g) no obvious diffusion restriction on DWI and corresponding ADC low map images

Conclusion

A wide variety of usual and unusual lesions exist in the CP angle. Signal intensity at MR imaging, enhancement, shape and margins, extent, mass effect, and adjacent bone reaction are helpful in establishing the diagnosis. MRI is considered as an excellent noninvasive investigation of the CPA lesions. It can identify the site and extension of the lesions as well as the characteristic signal. Apart from diagnosing, MR imaging plays an important role in stratifying patients into appropriate treatment options.

References

1. Imaging of the cerebellopontine angle. Lakshmi M, Glastonbury CM. Neuroimaging Clin N Am. 2009;19:393–406. doi: 10.1016/j.nic.2009.06.004.
2. Valavanis A, Schubiger O, Naidich T. Clinical imaging of the cerebellopontine angle. Berlin: Springer-Verlag; 1987.
3. Moffat DA, Ballagh RH. Rare tumours of the cerebellopontine angle. Clin Oncol. 1995; 7:28–41. doi: 10.1016/S0936-6555(05)80632-6.
4. Bartels LJ, Arrington JR. Rare tumors of the cerebellopontine angle. In: Jackler RK, Brackmann D, editors. Neurotology. St. Louis: Mosby; 1994. pp. 835–861.
5. Press GA, Hesselink JR. MR imaging of cerebellopontine angle and internal auditory canal lesions at 1.5 T. AJR. 1988;150(6):1371–1381. doi: 10.2214/ajr.150.6.1371.
6. Komatsuzaki A, Tsunoda A. Nerve origin of the acoustic neuroma. J Laryngol Otol. 2001;115(5):376–379. doi: 10.1258/0022215011907910.
7. Carlson M & Link M. Vestibular Schwannomas. N Engl J Med. 2021; 384(14): 1335-48. doi:10.1056/nejmra2020394.
8. Mulkens T, Parizel P, Martin J et al. Acoustic Schwannoma: MR Findings in 84 Tumors. AJR Am J Roentgenol. 1993;160(2):395-8. doi:10.2214/ajr.160.2.8424360.
9. Daniels DL, Millen SJ, Meyer GA, et al. MR detection of tumor in the internal auditory canal. AJR. 1987;148(6):1219–1222. doi: 10.2214/ajr.148.6.1219.
10. Held P, Fellner C, Seitz J, et al. The value of T2-weighted MR images for the diagnosis of acoustic neuromas. Eur J Radiol. 1999;30(3):237–244. doi: 10.1016/S0720-048X(98)00026-6.
11. Siegelman E, Mishkin M, Taveras J. Past, Present, and Future of Radiology of Meningioma. Radiographics. 1991;11(5):899-910. doi:10.1148/radiographics.11.5.1947324.
12. Ginsberg L. Radiology of Meningiomas. J Neuro-Oncol. 1996;29(3):229-38. doi:10.1007/bf00165653.
13. Osborn AG, editor. Meningiomas and other nonglial neoplasms. In: Diagnostic Neuroradiology. St. Louis: Mosby; 1994. p. 579-625.
14. Tsuruda J.S., Chew W.M., Moseley M.E., Norman D. Diffusion-weighted MR imaging of the brain: value of differentiating between extraaxial cysts and epidermoid tumors. AJR Am J Roentgenol. 17.1990;155:1059–1065. doi: 10.2214/ajr.155.5.2120936.
15. Ikushima I, Korogi Y, Hirai T, et al. MR of epidermoids with a variety of pulse sequences. AJNR Am J Neuroradiol 1997; 18:1359–1363.
16. Tampieri D., Melanson D., Ethier R. MR imaging of epidermoid cysts. AJNR Am J Neuroradiol. 1989; 10:351–356.
17. Dutt, Sunil N.; Mirza, Showkat; Chavda, Swarupsinh V; Irving, Richard M. Radiologic Differentiation of Intracranial Epidermoids from Arachnoid Cysts. Otology & Neurotology 23(1):84-92, January 2002.
18. Jallo GI, Woo HH, Meshki C, Epstein FJ, Wisoff JH. Arachnoid cysts of the cerebellopontine angle: Diagnosis and surgery. Neurosurgery. 1997; 40:31–7. doi: 10.1097/00006123-199701000-00006.
19. Alaani A, Hogg R, Siddiq MA, Chavda SV, Irving RM. Cerebellopontine angle arachnoid cysts in adult patients: what is the appropriate management? The Journal of Laryngology & Otology. 2005;119(5):337-341. doi:10.1258/0022215053945903.
20. Lipoma in the cerebellopontine angle. Steimlé R, Pageaut G, Jacquet G, Bourghli A, Godard J, Bertaud M.Surg Neurol. 1985 Jul;24(1):73-6. doi: 10.1016/0090-3019(85)90068-0. PMID: 3874440.
21. Cerebellopontine angle lipomas. Pensak ML, Glasscock ME 3rd, Gulya AJ, Hays JW, Smith HP, Dickens JR.Arch Otolaryngol Head Neck Surg. 1986 Jan;112(1):99-101. doi: 10.1001/archotol.1986.03780010101020.PMID: 3484424.
22. Truwit CL, Barkovich AJ. Pathogenesis of intracranial lipoma: an MR study in 42 patients. AJR Am J Roentgenol. 1990;155 (4): 855-64. AJR Am J Roentgenol (abstract) - Pubmed citation.